Inhomogeneous model colloid-polymer mixtures: Adsorption at a hard wall

J. M. Brader,[1] M. Dijkstra,[2] and R. Evans[1]
[1]*H.H. Wills Physics Laboratory, University of Bristol, Bristol BS8 1TL, United Kingdom*
[2]*Debye Institute, Soft Condensed Matter Physics, Utrecht University, Princetonpln 5, 3584 CC Utrecht, The Netherlands*
(Received 6 October 2000; published 27 March 2001)

We study the equilibrium properties of inhomogeneous model colloid-polymer mixtures. By integrating out the degrees of freedom of the ideal polymer coils, we derive a formal expression for the effective one-component Hamiltonian of the (hard sphere) colloids that is valid for arbitrary external potentials acting on both the colloids and the polymers. We show how one can recover information about the distribution of polymer in the mixture given knowledge of the colloid correlation functions calculated using the effective one-component Hamiltonian. This result is then used to furnish the connection between the free-volume and perturbation theory approaches to determining the bulk phase equilibria. For the special case of a planar hard wall the effective Hamiltonian takes an explicit form, consisting of zero-, one-, and two-body, but no higher-body, contributions provided the size ratio $q=\sigma_p/\sigma_c<0.1547$, where σ_c and σ_p denote the diameters of colloid and polymer respectively. We employ a simple density functional theory to calculate colloid density profiles from this effective Hamiltonian for $q=0.1$. The resulting profiles are found to agree well with those from Monte Carlo simulations for the same Hamiltonian. Adding very small amounts of polymer gives rise to strong depletion effects at the hard wall which lead to pronounced enhancement of the colloid density profile (close to the wall) over what is found for hard spheres at a hard wall.

DOI: 10.1103/PhysRevE.63.041405 PACS number(s): 82.70.Dd, 61.20.Gy, 68.43.Mn

I. INTRODUCTION

The addition of nonadsorbing polymers to a colloidal suspension gives rise to an attractive interaction between the colloidal particles. The physical mechanism for this phenomenon is the depletion effect whereby an effective attractive interaction is induced between the colloids due to the exclusion of polymer from a depletion zone between these; the range of the interaction is set by the diameter of the polymer coils and the strength of the attraction determined by the chemical potential of the polymer reservoir [1]. A popular simple model of the binary colloid-polymer mixture treats the colloids as hard spheres, with diameter σ_c, and the polymers as ideal interpenetrating coils as regards their mutual interactions but which are excluded by a center of mass distance $(\sigma_c+\sigma_p)/2$ from the colloids [1,2]. It was shown previously [3] that, for such a homogeneous colloid-polymer mixture, explicitly integrating out the degrees of freedom of the polymer gives rise to an effective Hamiltonian for the colloids consisting of zero-, one-, two-, and higher-body terms. Use of this effective Hamiltonian has provided much insight into the phase equilibria [3–5] and structure [3,6,7] in bulk colloid-polymer mixtures. Surprisingly little attention has been paid to *inhomogeneous* colloid-polymer mixtures where the average density profiles of both species are spatially varying. Such situations arise in adsorption at a solid substrate, in mixtures confined in narrow pores, at the planar interface between two coexisting (colloid-rich and polymer-rich) fluid phases [8–10], and in colloidal crystals. In these situations it is not evident that the mapping from an inhomogeneous binary mixture to an inhomogeneous effective one-component fluid (of colloids) is tractable, i.e., will lead to an effective Hamiltonian that is sufficiently simple to employ in simulations or tackle by standard liquid state theories. Recall that direct simulation of the model binary mixture, which constitutes a very asymmetric, nonadditive system, is prohibited by slow equilibration, since huge numbers of polymer molecules are required per colloid particle at state points of interest. In this paper, we show that the integrating out procedure can be carried through for an inhomogeneous colloid-polymer mixture, subject to external potentials that break translational invariance. The presence of external potentials gives rise to terms in the effective Hamiltonian representing additional depletion effects, which have important consequences for the application of effective Hamiltonians to inhomogeneous problems, in particular, to the study of adsorption, confined fluids, and fluid interfaces. For highly asymmetric mixtures, with size ratio $q\equiv\sigma_p/\sigma_c<0.1547$, near a planar hard wall the effective Hamiltonian reduces to a particularly simple form consisting of zero-, one-, and two-body contributions but no higher-body terms. It is identical to the Hamiltonian derived for the bulk system [3] apart from an additional, attractive one-body term arising from depletion of polymer at the hard wall. We employ this effective Hamiltonian in an approximate density functional treatment (DFT) and in a Monte Carlo simulation study of the density profile of colloids at a hard wall in mixtures with size ratio $q=0.1$. To the best of our knowledge this is the first investigation of the effects of depletion on colloid adsorption in such a model mixture.

Once the degrees of freedom of the polymer coils have been integrated out, it might seem as though information about the distribution of polymer has been lost. However, given knowledge of the colloid correlation functions obtained from the effective Hamiltonian, a formally exact expression for the density profile of the polymers can be derived. This can be usefully employed for the calculation of both homogeneous (the polymer concentration in the bulk mixture) and inhomogeneous (interfacial) profiles.

The paper is organized as follows. In Sec. II we describe

the model and show how the polymer degrees of freedom can be integrated out to yield an effective Hamiltonian in the presence of arbitrary external potentials. We then specialize to the case where the external potentials represent a hard wall and show that explicit expressions can be derived for the various terms in the Hamiltonian. In Sec. III we show how it is possible to recover information about the distribution of the polymer and use the formalism to furnish the connection between the free-volume [5] and perturbation/integral-equation theories [3,4] of the free-volume fraction and the phase equilibria, which has hitherto been lacking. Section IV A discusses sum rules for the colloid and polymer profiles at contact with a hard wall; these are generalizations of well-known sum rules for simple (atomic) fluids to the present effective Hamiltonian. Section IV B describes the results of our DFT calculations and simulation studies. We find that the two approaches lead to very similar colloid density profiles. Adding only small amounts of polymer (to the reservoir) leads to dramatic changes in the colloid profile, especially close to the hard wall where depletion increases the contact value to many times its value in the absence of polymer, i.e., the value appropriate to a pure hard sphere fluid at a hard wall. We conclude in Sec. V with a summary and discussion of the possible relevance of our results for adsorption phenomena in real colloidal systems.

II. THE EFFECTIVE HAMILTONIAN FOR AN INHOMOGENEOUS COLLOID-POLYMER MIXTURE

We consider an extreme nonadditive binary hard sphere mixture consisting of N_c hard spheres, representing colloid, and N_p interpenetrable, noninteracting particles, representing ideal polymer in a volume V at temperature T. This provides a reasonable model of a colloid-polymer mixture as the interaction between sterically stabilized colloidal particles can be made close to that of hard spheres, and dilute solutions of polymer in a θ solvent are very weakly interacting. We implicitly assume that any solvent molecules that are present in a real suspension can be treated as an inert continuum, and thus have no effect on bulk or interfacial properties. The colloids interact via the hard sphere potential with a diameter σ_c and the polymer particles are excluded from the colloids to a center of mass distance of $(\sigma_c+\sigma_p)/2$, where the diameter $\sigma_p=2R_g$, with R_g the radius of gyration of the polymer coils. This simple model of an idealized colloid-polymer mixture is often called the Asakura-Oosawa (AO) model [1] although it was first defined explicitly by Vrij [2]. It is specified by the pair potentials

$$\phi_{cc}(R_{ij})=\begin{cases}\infty & \text{for } R_{ij}<\sigma_c\\ 0 & \text{otherwise,}\end{cases}$$

$$\phi_{cp}(|\mathbf{R}_i-\mathbf{r}_j|)=\begin{cases}\infty & \text{for } |\mathbf{R}_i-\mathbf{r}_j|<\frac{1}{2}(\sigma_c+\sigma_p)\\ 0 & \text{otherwise,}\end{cases}$$

$$\phi_{pp}(r_{ij})=0, \tag{1}$$

where $\mathbf{R}$ and $\mathbf{r}$ denote colloid and polymer center of mass coordinates, respectively, with $R_{ij}=|\mathbf{R}_i-\mathbf{R}_j|$ and $r_{ij}=|\mathbf{r}_i-\mathbf{r}_j|$. The Hamiltonian thus consists of (trivial) kinetic energy contributions and a sum of interaction terms $H=H_{cc}+H_{cp}+H_{pp}$, where

$$H_{cc}=\sum_{i<j}^{N_c}\phi_{cc}(R_{ij}),$$

$$H_{cp}=\sum_{i}^{N_c}\sum_{j}^{N_p}\phi_{cp}(|\mathbf{R}_i-\mathbf{r}_j|), \tag{2}$$

$$H_{pp}=\sum_{i<j}^{N_p}\phi_{pp}(r_{ij})=0.$$

Following Ref. [3] we work in a semi-grand-canonical, (N_c,z_p,V,T), ensemble in which the fugacity of the polymers, $z_p=\Lambda_p^{-3}\exp(\beta\mu_p)$, is fixed, μ_p denotes the chemical potential of the reservoir of polymer, and $\beta=1/k_BT$. Here, in addition to the pairwise interactions we add two, in general different, external fields which couple independently to the colloid and polymer degrees of freedom:

$$V_c^{\text{ext}}=\sum_{i}^{N_c}v_c^{\text{ext}}(\mathbf{R}_i),\quad V_p^{\text{ext}}=\sum_{i}^{N_p}v_p^{\text{ext}}(\mathbf{r}_i). \tag{3}$$

The quantity of interest is the Helmholtz free energy $F(N_c,V,z_p)$, which in the semi-grand-canonical ensemble is given by

$$\exp[-\beta F]=\sum_{N_p=0}^{\infty}\frac{z_p^{N_p}}{N_p!N_c!\Lambda_c^{3N_c}}\int d\mathbf{r}^{N_p}\times\exp[-\beta(H_{cc}+H_{cp}+V_c^{\text{ext}}+V_p^{\text{ext}})], \tag{4}$$

where Λ_ν is the thermal de Broglie wavelength of species ν and we have used the fact that $H_{pp}=0$. In order to integrate out the degrees of freedom of the polymer coils, this expression must first be rewritten in a form that resembles the Helmholtz free energy of a one-component system of colloids interacting via an effective Hamiltonian $H^{\text{eff}}\equiv H_{cc}+\Omega+V_c^{\text{ext}}$. The effective potential Ω describes how the interactions between the colloids are modified by the presence of the polymer and represents the grand potential of the ideal polymer coils in the presence of both the applied external field V_p^{ext} and the external field of a fixed configuration of N_c colloids, i.e., the partitiion function for N_c colloids is

$$Z\equiv\exp[-\beta F]=\frac{1}{N_c!\Lambda_c^{3N_c}}\int d\mathbf{R}^{N_c}\exp[-\beta(H_{cc}+\Omega+V_c^{\text{ext}})], \tag{5}$$

where

$$\exp[-\beta\Omega]\equiv\sum_{N_p=0}^{\infty}\frac{z_p^{N_p}}{N_p!}\int d\mathbf{r}^{N_p}\exp[-\beta(H_{cp}+V_p^{\text{ext}})]. \tag{6}$$

It is clear that, in general, the effective potential $\Omega \equiv \Omega(\{\mathbf{R}^{N_c}\})$ is still many body in character, because the free volume available to the polymer coils, on which it depends, is different for each configuration $\{\mathbf{R}^{N_c}\}$ of the N_c colloids. The essential simplification provided by this model is that, because the polymer coils are noninteracting, both H_{cp} and V_p^{ext} appear in Eq. (6) as external (one-body) fields. If the polymers were allowed to interact, as is the case for a binary hard sphere mixture, then the Boltzmann factor would contain an additional term H_{pp}, which would complicate the analysis considerably—see below. As both H_{cp} and V_p^{ext} appear as external fields, the right hand side of Eq. (6) can be expressed as an exponential:

$$\begin{aligned}\exp[-\beta\Omega] &= \sum_{N_p=0}^{\infty} \frac{z_p^{N_p}}{N_p!} \left\{ \int d\mathbf{r}_j \right. \\ &\quad \times \exp\left[-\beta \left(\sum_{i=1}^{N_c} \phi_{cp}(|\mathbf{R}_i - \mathbf{r}_j|) \right.\right. \\ &\quad \left.\left. + v_p^{\text{ext}}(\mathbf{r}_j) \right) \right] \Bigg\}^{N_p} \\ &= \exp\left\{ z_p \int d\mathbf{r}_j \exp\left[-\beta \left(\sum_{i=1}^{N_c} \phi_{cp}(|\mathbf{R}_i - \mathbf{r}_j|) \right.\right.\right. \\ &\quad \left.\left.\left. + v_p^{\text{ext}}(\mathbf{r}_j) \right) \right] \right\}. \end{aligned} \tag{7}$$

In order to evaluate this expression we expand the integral in terms of the Mayer function of the colloid-polymer interaction potential, $f_{ij} \equiv f(|\mathbf{R}_i - \mathbf{r}_j|) \equiv \exp[-\beta\phi_{cp}(|\mathbf{R}_i - \mathbf{r}_j|)] - 1$. For a hard sphere interaction f_{ij} is simply a step function, thus allowing a geometrical interpretation to be given to the resulting integrals. Performing the cluster expansion yields

$$\begin{aligned} -\beta\Omega &= z_p \int d\mathbf{r}_j e_j \prod_{i=1}^{N_c} (1 + f_{ij}) \\ &= z_p \int d\mathbf{r}_j e_j + \sum_{i=1}^{N_c} z_p \int d\mathbf{r}_j f_{ij} e_j \\ &\quad + \sum_{i<k}^{N_c} z_p \int d\mathbf{r}_j f_{ij} f_{kj} e_j + \cdots, \end{aligned} \tag{8}$$

where $e_j \equiv \exp[-\beta v_p^{\text{ext}}(\mathbf{r}_j)]$ is the Boltzmann factor of the polymer external potential. Although this procedure is similar in spirit to a standard virial expansion, it is not a density expansion because all terms are linear in the fugacity of the polymer as a result of the exponentiation in Eq. (7). Note that for an ideal polymer $z_p = \beta P_p^r = \rho_p^r(z_p)$, where P_p^r and ρ_p^r are the pressure and density of the polymer reservoir, respectively. Equation (8) can be written in diagrammatic terms [11] as

$-\beta\Omega$ = 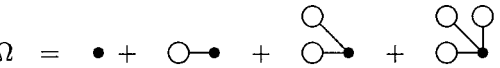 + $\cdots$, (9)

where (i) each black circle represents a factor of z_p, and an integral over volume V weighted with a factor $\exp[-\beta v_p^{\text{ext}}]$, and (ii) each open circle represents an f bond and a sum over the colloid coordinates. If the polymers were allowed to interact then this expansion would immediately become much more complicated as it would also involve polymer-polymer Mayer bonds. A full diagrammatic expansion of Ω for a *homogeneous* mixture with arbitrary (pairwise) interactions can be found in Ref. [12] where the formalism is applied in the context of binary hard sphere mixtures. Each term in the effective potential Ω can then be classified according to the number $n = 0,1,2,\ldots,N_c$ of colloids that interact simultaneously with the sea of ideal polymer:

$$\beta\Omega = \sum_{n=0}^{N_c} \beta\Omega_n. \tag{10}$$

First, we review the evaluation of Ω for a homogeneous system for which $v_p^{\text{ext}}(\mathbf{r}_{ij}) = 0$, i.e., $e_j \equiv 1$. It follows that $-\beta\Omega_0^{\text{bulk}} = z_p V$ and $-\beta\Omega_1^{\text{bulk}} = -z_p N_c \pi(\sigma_c + \sigma_p)^3/6 = -z_p \eta_c (1+q)^3 V$, where $\eta_c = (\pi/6)\sigma_c^3 N_c / V$ is the colloid packing fraction and $q \equiv \sigma_p/\sigma_c$, is the size ratio [3]. For the homogeneous system the one-body term Ω_1 is a constant, independent of the colloid coordinates; however, as we shall see, this is not generally the case, and for inhomogeneous systems Ω_1 acquires a spatial dependence determined by the external potential. The integral required for $-\beta\Omega_2^{\text{bulk}}$ is simply the convolution of two excluded volume spheres, given by the volume of a lens shaped region, multiplied by z_p. Thus we find $\Omega_2^{\text{bulk}} = \Sigma_{i<j} \phi_{\text{AO}}(R_{ij})$ where $\phi_{\text{AO}}(R)$ is the familiar Asakura-Oosawa pair potential, given by

$$\beta\phi_{\text{AO}}(R) = \begin{cases} -\dfrac{\pi}{6}\sigma_p^3 z_p \dfrac{(1+q)^3}{q^3} \left\{ 1 - \dfrac{3R}{2(1+q)\sigma_c} + \dfrac{R^3}{2(1+q)^3\sigma_c^3} \right\}, & \sigma_c < R < \sigma_c + \sigma_p \\ 0, \quad R > (\sigma_c + \sigma_p). \end{cases} \tag{11}$$

It should be noted that Eq. (8) for Ω admits any configuration of the colloids, since it contains no information about H_{cc} or V_c^{ext}. However, because all physical properties come from the substitution of Eq. (8) into Eq. (5), unphysical configurations where colloids overlap are unimportant. Identical considerations also apply to all higher-body terms. One of the most attractive features of the present model is that geometrical arguments can be used to show that when the size ratio $q < 2/\sqrt{3} - 1 = 0.1547$, all three- and higher-body contributions to Ω are identically zero, i.e., $\Omega_{n>2} \equiv 0$. This corre-

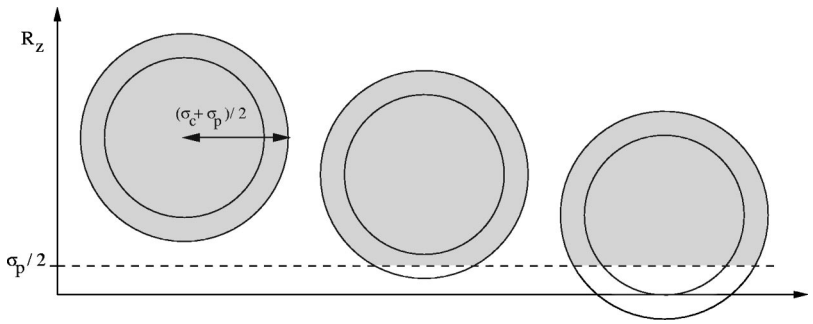

FIG. 1. The shaded region contributes to the one-body integral in Eq. (8). When the position of the center of the colloid $R_z \geqslant (1/2)(\sigma_c+2\sigma_p)$ the entire exclusion sphere contributes, but for $R_z<(1/2)(\sigma_c+2\sigma_p)$ overlap with the polymer exclusion layer of thickness $\sigma_p/2$ at the wall introduces a spatial dependence.

sponds to a situation where there can be no triple overlap of excluded volume regions, even when three colloids are in simultaneous contact. As a result, there exists an exact mapping [3,7] between the full two-component AO mixture and the effective one-component system of colloids interacting via the effective bulk Hamiltonian $\Omega_0^{\rm bulk}+\Omega_1^{\rm bulk}+\Omega_2^{\rm bulk}+H_{cc}$. In calculating thermodynamic quantities from the effective Hamiltonian one must be careful to take into account the effects of the zero- and one-body terms $\Omega_0^{\rm bulk}$ and $\Omega_1^{\rm bulk}$, which are often neglected. As both of these terms are independent of colloid coordinates $\{\mathbf{R}^{N_c}\}$ they have no effect on the equilibrium structure of the effective one-component system. However, as these terms are linear in V and N_c, respectively, they do contribute to shifts in both the pressure and chemical potential and provide substantial contributions to the total compressibility of the mixture, making this very different from the osmotic compressibility calculated directly from the effective Hamiltonian [7]. Note that these terms have no effect on the phase equilibria of the mixture [12].

If we now turn to the inhomogeneous situation where both $v_c^{\rm ext}$ and $v_p^{\rm ext}$ are nonzero, Eq. (8) still provides an exact expression for the effective Hamiltonian; all that remains is to specify $v_p^{\rm ext}$. For the purpose of illustration let us specialize to the simplest possible case where both $v_c^{\rm ext}$ and $v_p^{\rm ext}$ represent a planar hard wall located in the x-y plane:

$$v_c^{\rm ext}(R_z)=\begin{cases}\infty, & R_z<\frac{1}{2}\sigma_c\\ 0, & R_z\geqslant\frac{1}{2}\sigma_c,\end{cases}\qquad v_p^{\rm ext}(r_z)=\begin{cases}\infty, & r_z<\frac{1}{2}\sigma_p\\ 0, & r_z\geqslant\frac{1}{2}\sigma_p.\end{cases} \tag{12}$$

We now proceed to evaluate the integrals in Eq. (8) one at a time. The zero-body term $-\beta\Omega_0$ is simply z_pV, the same as in bulk. The one-body term $\beta\Omega_1$, however, is now a function of the z component of the colloid center coordinate R_z. This dependence arises from the presence of the Boltzmann factor e_j in the integrand, which for a hard wall interaction is simply a step function. The only contribution to Ω_1 comes from the shaded volume shown in Fig. 1. Thus for $R_z\geqslant\frac{1}{2}(\sigma_c+2\sigma_p)$, $\Omega_1=\Omega_1^{\rm bulk}$, whereas for $R_z<\frac{1}{2}(\sigma_c+2\sigma_p)$ overlap with the polymer exclusion layer reduces the shaded volume and we find

$$\Omega_1(R_z)=\Omega_1^{\rm bulk}+\sum_{i=1}^{N_c}\phi_{\rm AO}^{\rm wall}(R_{zi}), \tag{13}$$

where the one-body potential

$$\beta\phi_{\rm AO}^{\rm wall}(\tilde{z})=\begin{cases}-\dfrac{1}{6}\sigma_p^3 z_p\dfrac{1}{2q^3}[2(q-\tilde{z})+1][(3+q)q-\frac{1}{2}(3-q)(2\tilde{z}-1)-\frac{1}{2}(2\tilde{z}-1)^2] & \text{for } \frac{1}{2}\sigma_c<R_z<\frac{1}{2}(\sigma_c+2\sigma_p)\\ 0 \quad \text{otherwise,}\end{cases} \tag{14}$$

and where $\tilde{z}\equiv R_z/\sigma_c$. This is the familiar Asakura-Oosawa depletion potential between a single colloid and a planar hard wall. Note that $\phi_{\rm AO}^{\rm wall}$ has range σ_p and a similar shape to the AO pair potential $\phi_{\rm AO}$; it constitutes an attractive potential well at the wall. The depletion of polymer at the hard wall always produces an effective wall-colloid attraction. It is expected, therefore, that the colloids will be preferentially adsorbed by a hard wall. Once again it is worth noting that the integral for Ω_1 permits any value of R_z but substitution into Eq. (5) eliminates unphysical configurations of colloid. If we turn now to the two-body term Ω_2, the value of the required integral is given by the shaded volume shown in Fig. 2. In general, when a pair of colloids are close to the wall, the two-body term in Eq. (8) no longer yields the bulk Asakura-Oosawa expression as there exists a region of triple overlap between the colloid-colloid lens and the polymer exclusion layer [see Fig. 2(a)], which does not contribute to the integral. The two-body potential thus becomes a complicated function of $\mathbf{R}_1$ and $\mathbf{R}_2$ and not simply a function of the separation $|\mathbf{R}_1-\mathbf{R}_2|$. However, simple geometrical arguments can be used to show that for $q<0.25$ all Ω_n for $n\geqslant 2$ are unaltered from their bulk forms in the presence of

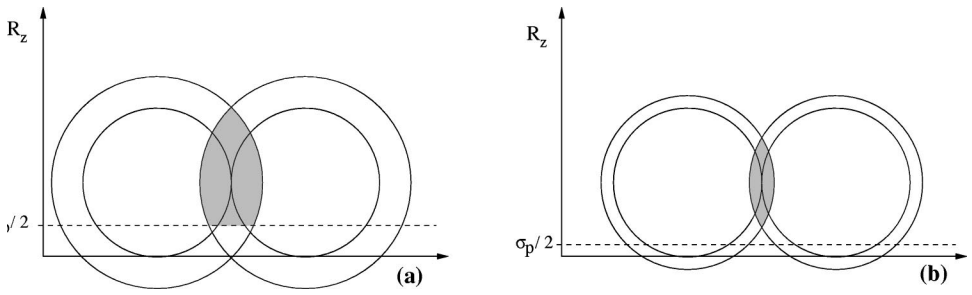

FIG. 2. The shaded region contributes to the two-body term in Eq. (8). For larger size ratios (a) the exclusion lens between colloids overlaps with the polymer exclusion layer at the wall and the two-body potential becomes a complicated function. However, for size ratios $q<0.25$ (b) this triple overlap cannot occur and so the bulk Asakura-Oosawa pair potential, given by the volume of the lens, remains valid in the interfacial region.

the hard wall. Physically, this corresponds to a situation where the exclusion layer at the wall and the colloid-colloid exclusion lens cannot overlap, even when the colloids are in contact with the wall; see Fig. 2(b). Thus, for $q<0.25$, we are left with an effective one-component Hamiltonian for a fluid of colloids near a hard wall that has the form

$$H^{\mathrm{eff}}=\Omega_0^{\mathrm{bulk}}+\Omega_1^{\mathrm{bulk}}+H_{cc}+\sum_i^{N_c} v_c^{\mathrm{ext}}(R_{zi})+\sum_i^{N_c} \phi_{\mathrm{AO}}^{\mathrm{wall}}(R_{zi})$$

$$+\sum_{i<j} \phi_{\mathrm{AO}}(R_{ij})+\text{higher-body terms}, \tag{15}$$

where the higher-body terms are identical to those in bulk. It follows that for $q<0.1547$ all of the higher-body terms become identically zero, and the effective Hamiltonian H^{eff} is exact when truncated after the pairwise term. Thus for q below this critical size ratio there exists an exact mapping between the partition function of the *inhomogeneous* mixture and that of the effective one-component system of colloids described by the truncated H^{eff}. This Hamiltonian differs from that in bulk only by the addition of the one-body depletion-induced attractive potential $\phi_{\mathrm{AO}}^{\mathrm{wall}}$ and the hard wall external potential V_c^{ext}. Note that the polymer manifests itself in H^{eff} solely through the dependence of Ω_0^{bulk}, Ω_1^{bulk}, $\phi_{\mathrm{AO}}^{\mathrm{wall}}$, and ϕ_{AO} on the polymer fugacity z_p. Although we have taken the case of a planar hard wall as an example, there are many other external potentials for which the above procedure could be usefully employed.

At this stage it is appropriate to consider the situation of spontaneously generated inhomogeneities where the density profiles of colloid and polymer are spatially varying in the absence of external fields. Examples are the planar interface between demixed fluid phases [13,10] and colloidal crystals where the densities vary periodically. In such cases H^{eff} reduces to the effective Hamiltonian of the bulk system; there are no additional contributions associated with the inhomogeneity. At first sight this may seem somewhat surprising, as the distribution of polymer in a colloidal crystal, or in the region of the fluid-fluid interface, is clearly very different from that in a bulk fluid, and one might imagine that different effective interactions might arise. However, because we work exclusively with a reservoir of polymer, it is the fugacity z_p of this reservoir that provides the only parameter by which we can tune the interactions in the system. As z_p is constant throughout an inhomogeneous fluid, then so too is the effective interaction between the colloids, regardless of the local polymer density. This serves to reinforce the fact that the species that is integrated out is treated grand canonically.

III. OBTAINING THE POLYMER DISTRIBUTION FROM THE EFFECTIVE HAMILTONIAN

A. Inhomogeneous case

Using the effective Hamiltonian H^{eff} derived in the previous section one may treat the colloids as an effective one-component system with given interactions and subject to an external field. Once the effective Hamiltonian has been specified one is completely free to choose how to tackle the statistical mechanics of the effective one-component system. Thus, using a theory or a simulation of a one-component fluid it is possible, in principle, to calculate any of the required equilibrium properties of the colloidal particles. However, it would seem that by adopting an effective Hamiltonian for the colloids all information about the distribution of the polymer has been lost; the polymer degrees of freedom have been integrated out. On the other hand, by using the effective Hamiltonian, we have obtained information about the properties of the colloids and so, returning to the original problem, in which both species are treated on an equal footing, we should be in a better position to calculate the properties of the polymer; half of the problem has already been solved. In order to recover information about the polymer distribution we make use of the standard functional relation

$$\rho_p^{(1)}(\mathbf{r})=\frac{\delta F[v_p^{\mathrm{ext}}]}{\delta v_p^{\mathrm{ext}}(\mathbf{r})}, \tag{16}$$

which is easily derived by taking the functional derivative in Eq. (4) [14]. If, however, we use Eq. (5) in order to perform this functional derivative, where the partition function Z has been written in one-component form, then it is clear that the only quantity in this expression that is a functional of v_p^{ext} is the effective potential $\Omega\equiv\Omega(\{\mathbf{R}^{N_c}\};[v_p^{\mathrm{ext}}])$. Taking the functional derivative yields

$$\rho_p^{(1)}(\mathbf{r}) = \frac{1}{Z}\frac{1}{N_c!\Lambda_c^{3N_c}}\int d\mathbf{R}^{N_c}\frac{\delta\Omega(\{\mathbf{R}^{N_c}\};[v_p^{\rm ext}])}{\delta v_p^{\rm ext}(\mathbf{r})} \times \exp[-\beta(H_{cc}+\Omega+V_c^{\rm ext})]. \quad (17)$$

Now, as Ω consists of a sum of terms as given in Eq. (10) the polymer profile can also be written as a sum of terms, each of which is the average over the colloids (at fixed fugacity of the polymer reservoir) of the functional derivative of a term in the effective potential:

$$\rho_p^{(1)}(\mathbf{r}) = \left\langle \frac{\delta\Omega_0[v_p^{\rm ext}]}{\delta v_p^{\rm ext}(\mathbf{r})}\right\rangle_{z_p} + \left\langle \frac{\delta\Omega_1[v_p^{\rm ext}]}{\delta v_p^{\rm ext}(\mathbf{r})}\right\rangle_{z_p} + \left\langle \frac{\delta\Omega_2[v_p^{\rm ext}]}{\delta v_p^{\rm ext}(\mathbf{r})}\right\rangle_{z_p} + \cdots. \quad (18)$$

This expression is valid for any binary mixture with integrable pairwise interactions. Moreover, it is easily generalized to an arbitrary number of species. We now specialize to the Asakura-Oosawa model, where each term in the expansion of Ω is given by a simple integral and the functional dependence is explicit. For this model the first term of Eq. (18) is given by $z_p \exp[-\beta v_p^{\rm ext}(\mathbf{r})]$ and is independent of the colloid distribution. The second term is slightly more complicated and incorporates information about the volume from which the polymers are excluded due to the presence of individual colloids; it thus requires the equilibrium density profile $\rho_c^{(1)}$ of the colloids as input. It is important to note that the required colloidal density profile must be calculated using the effective Hamiltonian (15). As might be expected, the two-body term involves the inhomogeneous pair correlation function $\rho_c^{(2)}$ of a system of colloids interacting via the effective Hamiltonian (15), and includes information about the effect of correlations between pairs of colloids on the (local) free volume available to the polymer. This procedure can be continued to generate an exact expression for the polymer profile, which, in general, requires knowledge of all *n*-body correlation functions of the colloids, calculated using the effective Hamiltonian. The resulting expression for the polymer profile is given by

$$\rho_p^{(1)}(\mathbf{r}) = z_p \exp[-\beta v_p^{\rm ext}(\mathbf{r})]\Big(1 + \int d\mathbf{R}_2 f_{cp}(\mathbf{r}-\mathbf{R}_2)\rho_c^{(1)}(\mathbf{R}_2) + \tfrac{1}{2}\int d\mathbf{R}_2\int d\mathbf{R}_3 f_{cp}(\mathbf{r}-\mathbf{R}_2) f_{cp}(\mathbf{r}-\mathbf{R}_3) \times \rho_c^{(2)}(\mathbf{R}_2,\mathbf{R}_3)+\cdots\Big). \quad (19)$$

This expression is valid for arbitrary external potentials $v_p^{\rm ext}$ and $v_c^{\rm ext}$, but is of limited use for large size ratios since it requires higher-order correlation functions of the colloids, which are difficult to obtain from the effective Hamiltonian. The usefulness of Eq. (19) becomes evident for smaller size ratios where geometrical arguments, similar to those used previously, show that for $q<0.1547$ all terms involving $\rho_c^{(n)}$ for $n\geqslant 3$ are identically zero and so the highest-order correlation function required is $\rho_c^{(2)}$. For very small size ratios, say $q<0.1$, the first two terms are expected to dominate and the polymer profile is primarily determined by the exclusion volume due to individual colloids. In these circumstances one might employ simulation data for $\rho_c^{(1)}$ in order to make an estimate of the polymer profile.

B. Bulk case

In order to use Eq. (19) for inhomogeneous situations, even for $q<0.1547$, one is required to calculate the two-body correlation function $\rho_c^{(2)}(\mathbf{R}_1,\mathbf{R}_2)$, which is not easy to obtain either from simulation or from theory. However, in a bulk fluid this function reduces to $\rho_c^2 g_{cc}(R_{12};\rho_c,z_p)$ where $\rho_c = N_c/V$ is the number density of the colloid and $g_{cc}(R_{12};\rho_c,z_p)$ is the colloid-colloid radial distribution function. Equation (19) can be simplified to yield a useful expression for the actual density ρ_p of polymer in the system at given fugacity z_p of the polymer reservoir and given η_c. By a simple change of variable Eq. (19) reduces to the following bulk expression:

$$\rho_p/\rho_p^r = 1-\eta_c(1+q)^3 - \frac{12\eta_c^2 q^3}{\eta_p^r}\int_1^{1+q} dr\, r^2 g_{cc}(r;\rho_c,z_p)\beta\phi_{\rm AO}(r)+\cdots, \quad (20)$$

where $r\equiv R_{12}/\sigma_c$ and $\eta_p^r = \pi\rho_p^r\sigma_p^3/6$ is the packing fraction of the polymer in the reservoir. It is important to note that the averages in Eq. (20) are taken over all configurations of the colloids interacting via the bulk effective Hamiltonian. If the averages were taken using merely the ''bare'' hard sphere colloid-colloid interaction ϕ_{cc}, then the effect of the polymer on the colloid distribution would be neglected; it is this information that is contained in $g_{cc}(r;\rho_c,z_p)$ and in the higher-order correlation functions entering the higher-order terms in Eq. (20). For $q<0.1547$ the higher-order terms vanish and Eq. (20) provides an explicit and exact expression for the free-volume fraction α of a colloid-polymer mixture, defined by

$$\alpha(\rho_c;z_p)\equiv\rho_p/\rho_p^r. \quad (21)$$

The theory requires as input the radial distribution function of the colloids, g_{cc}, which can be readily obtained from simulation or integral equation theories of the effective one-component bulk system described by the pair potential $\phi_{cc}(R)+\phi_{\rm AO}(R)$.

Equation (20) for α provides the connection between the free-volume [5] and perturbation/integral-equation theories [3,4] of the bulk phase equilibria. In order to determine the thermodynamic properties of a homogeneous system from knowledge of the bulk pair correlation functions three independent routes are available, namely, the virial, compressibility, and internal energy equations. The quantity of interest in determining the phase equilibria is the Helmholtz free energy F which is conveniently obtained within the internal energy route by the integration

$$\frac{\beta F(\rho_c;\lambda=1)}{V}=\frac{\beta F_0(\rho_c;\lambda=0)}{V}+\frac{1}{2}\rho_c^2\int_0^1 d\lambda\int_0^\infty d\mathbf{R}\, g(R;\rho_c,\lambda)\beta\phi_1(R). \tag{22}$$

This is an exact expression for a one-component system interacting solely via a pair potential ϕ, which is usually divided into (repulsive) reference and (attractive) perturbation parts, $\phi=\phi_0+\lambda\phi_1$, where λ is a coupling constant that switches on the effect of the perturbation as its value increases from 0 to 1 [15]. Standard first-order perturbation theory is obtained from Eq. (22) if the λ dependence is neglected and $g(r;\rho_c,\lambda)$ is replaced by $g(r;\rho_c,\lambda=0)$. Such an approach is taken in several studies of phase equilibria [3] with the Asakura-Oosawa pair potential ϕ_{AO} taken as ϕ_1, and with $\phi_0=\phi_{cc}$, the bare hard sphere potential between colloids.

An alternative approach to calculating the bulk phase behavior is the free-volume approach of Lekkerkerker *et al.* [5], which appears to have a basis quite different from that given by Eq. (22). The free-volume theory for the free energy of a bulk colloid-polymer mixture can be derived by considering the identity

$$\beta F(N_c,V,z_p)=\beta F(N_c,V,z_p=0)+\int_0^{z_p}dz_p'\left(\frac{\partial\beta F(N_c,V,z_p')}{\partial z_p'}\right), \tag{23}$$

which can be written as

$$\frac{\beta F(\rho_c,z_p)}{V}=\frac{\beta F(\rho_c,z_p=0)}{V}-\int_0^{z_p}dz_p'\alpha(\rho_c;z_p'), \tag{24}$$

since from Eq. (4) the partial derivative is $-\langle N_p\rangle_{z_p}/z_p=-\alpha(\rho_c;z_p)V$, where $\langle N_p\rangle_{z_p}$ is the average number of polymers in the (N_c,V,z_p) ensemble and we have used Eq. (21) and the fact that $z_p=\rho_p^r$ for an ideal polymer. The partial derivative can also be obtained from Eqs. (5) and (8) and is given by

$$-\left(\frac{\partial\beta F(N_c,V,z_p)}{\partial z_p}\right)=\frac{\mathrm{Tr}_c\{\exp[-\beta H^{\mathrm{eff}}]\int d\mathbf{r}_j\Pi_{i=1}^{N_c}(1+f_{ij})\}}{\mathrm{Tr}_c\exp[-\beta H^{\mathrm{eff}}]}. \tag{25}$$

where Tr_c is short for the integral $\int d\mathbf{R}^{N_c}$ over the coordinates of the colloidal particles. Given the geometrical interpretation of the Mayer function f_{ij} for the colloid-polymer interaction, the right hand side of Eq. (25) can be interpreted as the average free volume available to the polymer at fixed fugacity of the polymer reservoir, $\langle V_{\mathrm{free}}\rangle_{z_p}\equiv\alpha V$. If we focus first on size ratios $q<0.1547$, where use of the effective Hamiltonian truncated at the Asakura-Oosawa pair potential term is exact, we can establish the connection between the free-volume and standard perturbation/integral equation theories by substituting α obtained from Eq. (20) into Eq. (24) and using the substitution $z_p'\to\lambda z_p$. This yields

$$\frac{\beta F(\rho_c;\lambda=1)}{V}=\frac{\beta F_0(\rho_c;\lambda=0)}{V}-z_p[1-\eta_c(1+q)^3]+\frac{1}{2}\rho_c^2\int_0^1 d\lambda\int_0^\infty d\mathbf{R}\, g_{cc}(R;\rho_c,\lambda)\beta\phi_{\mathrm{AO}}(R), \tag{26}$$

i.e., we simply recover Eq. (22) with an additional term $-z_p[1-\eta_c(1+q)^3]$ arising from the zero- and one-body terms. $F_0(\rho_c;\lambda=0)$ refers to the Helmholtz free energy of the hard sphere fluid of density ρ_c.

So far all is exact and we have merely demonstrated that utilizing Eq. (23) is equivalent to utilizing Eq. (22), the standard coupling constant integration for the free energy of a system described by a pairwise potential. In the approach of Ref. [5] $\alpha(\rho_c;z_p)$ is replaced by $\alpha(\rho_c;z_p=0)$, i.e., the free-volume fraction of a test polymer in the low-density limit, for which the scaled particle theory [17] provides a good approximation. It is straightforward to show that the resulting free-volume approximation for F reduces to the standard first-order perturbation theory result,

$$\frac{\beta F(\rho_c;\lambda=1)}{V}=\frac{\beta F_0(\rho_c;\lambda=0)}{V}-z_p[1-\eta_c(1+q)^3]+\frac{1}{2}\rho_c^2\int_0^\infty d\mathbf{R}\, g_{cc}(R;\rho_c,\lambda=0)\beta\phi_{\mathrm{AO}}(R) \tag{27}$$

with $g_{cc}(R;\rho_c,\lambda=0)$ the hard sphere radial distribution function given by a scaled particle approximation. Clearly, more accurate results for α for *fluid* states would be obtained by employing Eq. (20) with integral equation closures such as the Percus-Yevick that are known to yield $g_{cc}(R;\rho_c,\lambda)$ in excellent agreement with simulation [3]. Note that, although for $q<0.1547$ α is dominated by the term $1-\eta_c(1+q)^3$ for all (physical) values of η_c and one might expect the free-volume approximation (27) to be accurate, it is the *derivatives* of α with respect to η_c that determine phase coexistence. That is why the free-volume approximation and perturbation theory yield metastable fluid-fluid coexistence curves at unrealistically high η_c for $q=0.1$ [3]. If one determines the free energy from Eq. (26), using the Percus-Yevick approximation for $g_{cc}(R;\rho_c,\lambda)$, the resulting fluid-fluid coexistence curve is closer to that from simulation [16].

It is for larger size ratios, where the pair potential description is no longer exact, that the free-volume approximation is of greater interest. Using the scaled particle expression [17] for α, which is central to the free-volume approach, constitutes an approximate resummation of the full expansion (20). Thus the approximation captures some of the effects of three- and higher-body effective interactions, which are known to be important at larger size ratios. Precisely which effects are captured and which are not and how to improve

systematically upon the basic approximation that sets $\alpha(\rho_c;z_p)=\alpha(\rho_c;z_p=0)$ is not obvious.

An important feature of our approach is that it provides a means of obtaining the polymer density $\rho_p^{(1)}(\mathbf{r})$ in the presence of a *crystalline* array of colloids. Equation (19), truncated at the two-body term and with $v_p^{\rm ext}\equiv 0$, should remain valid for a bulk crystal provided $q<0.1547$. Given an approximation for $\rho_c^{(2)}$ in the crystal one can determine the polymer density from knowledge of the (periodic) colloid density $\rho_c^{(1)}(\mathbf{R})$. This result incorporates much more information about the distribution of colloid than does the free-volume formula where α is assumed to depend only on the (constant) average colloid density ρ_c, i.e., the same formula is used for the solid and fluid phases [3,5]. Formally we can write Eq. (19) as

$$\rho_p^{(1)}(\mathbf{r})=z_p^{\star}(\mathbf{r})\alpha(\mathbf{r};z_p), \tag{28}$$

where $z_p^{\star}(\mathbf{r})\equiv z_p\exp[-\beta v_p^{\rm ext}(\mathbf{r})]$ and $\alpha(\mathbf{r};z_p)=-\delta\beta F[v_p^{\rm ext}]/\delta z_p^{\star}(\mathbf{r})$ depends on the average spatial distribution of the colloids. The free energy can be obtained by integration and the final term in Eq. (23) is replaced by $-\int_0^{z_p}dz_p'\int d\mathbf{r}\,\alpha(\mathbf{r};z_p')\exp[-\beta v_p^{\rm ext}(\mathbf{r})]$. For the bulk colloidal crystal, where $v_p^{\rm ext}\equiv 0$, Eq. (28) reduces to $\rho_p^{(1)}(\mathbf{r})=\rho_p^r\alpha(\mathbf{r};z_p)$ and $\alpha(\mathbf{r};z_p)$ can be interpreted as the spatially varying free-volume fraction of polymer in the crystal. Note that Eq. (19) implies that if $\rho_c^{(1)}(\mathbf{r})$ is periodic then so is the one-body polymer profile $\rho_p^{(1)}(\mathbf{r})$.

We conclude this section by remarking that an equivalent procedure can be developed for additive binary hard sphere mixtures. However, in this case the depletion pair potential and the higher-body potentials are not known explicitly so that each term in the effective Hamiltonian is known only approximately [12]. Moreover, truncation at the pair potential term is no longer exact for any size ratio since interactions between the small spheres (nonvanishing small-small Mayer function) can mediate many-body effective colloid interactions at all values of q. Thus, in principle, one should always employ the full n-body expansion. In practice, for small size ratios $q\leqslant 0.1$, α is given rather accurately by the expansion truncated after the zero-and one-body terms and for $q\leqslant 0.2$ the main features of the bulk phase behavior are well described by an effective Hamiltonian that incorporates only the pair potential contribution [12].

IV. THE MIXTURE NEAR A HARD WALL

A. Sum rules for contact densities

In this section we specialize to the colloid-polymer (AO) mixture near a planar hard wall described by the external potentials (12) and consider the density profiles $\rho_c(z)$ and $\rho_p(z)$. Henceforward, for ease of notation, we replace the colloid z coordinate R_z by z. It is well known that for any one-component fluid near a hard wall the contact density ρ_w satisfies the sum rule $\rho_w=\beta P$, where P is the pressure of the bulk (reservoir) fluid far from the wall. This sum rule provides a useful test for the reliability of theories and for the accuracy of simulations. For example, it is obeyed by non-local density functional treatments of the inhomogeneous fluid but is not obeyed by the standard closure approximations to the wall-particle Ornstein-Zernike equation [18]. For the case of a binary mixture near a hard wall the sum rule generalizes to $\sum_{\nu=1,2}\rho_{w\nu}=\beta P$, i.e., the sum of the contact densities is proportional to the (total) pressure of the bulk mixture. Rickayzen [19] has shown that it is possible to define a normal pressure P_ν for each species ν such that $\rho_{w\nu}=\beta P_\nu$. Each P_ν is given by a bulk fluid virial-like equation. However, P_ν cannot be expressed in terms of direct correlation functions and is therefore not amenable to calculation within DFT.

If we treat our AO mixture as a binary fluid it follows that the sum of contact densities must satisfy

$$\rho_{wc}+\rho_{wp}=\beta P \tag{29}$$

with $\rho_{wc}\equiv\rho_c(\sigma_c^+/2)$ and $\rho_{wp}\equiv\rho_p(\sigma_p^+/2)$. On the other hand, if we make the mapping to an effective one-component fluid of colloids and consider the case $q<0.25$, where integrating out the polymer at the hard wall yields the additional wall-colloid depletion potential (14) but no other inhomogeneous contribution, we can integrate the equation of hydrostatics [18] to obtain

$$\rho_{wc}-\beta\int_{\sigma_c^+/2}^{\infty}dz\,\rho_c(z)\frac{d\phi_{\rm AO}^{\rm wall}(z)}{dz}=\beta P_N(\infty), \tag{30}$$

where $P_N(\infty)$ is the normal component of the pressure far from the wall. Note that the integrand in Eq. (30) is zero for $z\geqslant(\sigma_c+2\sigma_p)/2$—see Eq. (14). It remains to identify $P_N(\infty)$. This quantity should be identified with the virial pressure of the bulk one-component fluid which, in turn, corresponds to the osmotic pressure $\Pi(\rho_c;z_p)$. Thus,

$$P_N(\infty)=\Pi(\rho_c;z_p)\equiv-\left(\frac{\partial A}{\partial V}\right)_{N_c,z_p}, \tag{31}$$

where $\exp[-\beta A]=\mathrm{Tr}_c\exp[-\beta W]$ with

$$W(N_c,z_p;\{\mathbf{R}^{N_c}\})=\sum_{i<j}[\phi_{cc}(R_{ij})+\phi_{\rm AO}(R_{ij})]+\sum_{n>2}\Omega_n, \tag{32}$$

i.e., $A(\rho_c;z_p)$ is the Helmholtz free energy of the one-component system with an interaction Hamiltonian consisting of two- and higher-body interactions [7]. The total free energy $F=A-P_p^r(z_p)[1-\eta(1+q)^3]V$ so that the total pressure is the sum of the osmotic pressure and that of the polymer reservoir:

$$P=\Pi(\rho_c;z_p)+P_p^r(z_p). \tag{33}$$

Equations (29) and (30) can be combined using Eqs. (31) and (33) to yield

$$\rho_{wp}-\rho_p^r=-\beta\int_{\sigma_c^+/2}^{\infty}dz\,\rho_c(z)\frac{d\phi_{\rm AO}^{\rm wall}(z)}{dz}, \tag{34}$$

which is a sum rule giving the polymer contact density in terms of an integral of the colloid profile over the range of the wall-colloid depletion potential. This result is, of course, specific to the AO model in the regime $q<0.25$. In practice its usefulness for simulations will be restricted to $q<0.1547$ since only for these size ratios is the mapping to a pair potential Hamiltonian exact. Equation (30) should be satisfied by the colloid profiles calculated from simulation or from a nonlocal DFT for the effective one-component system, provided $q<0.1547$. We shall use it to examine the accuracy of our numerical results presented below.

B. Colloid density profiles from DFT and simulation

In order to calculate the colloid profile $\rho_c(z)$ we require a DFT for a one-component fluid in which the fluid-fluid pair potential $\phi_{cc}(R)+\phi_{\rm AO}(R)$ exhibits a deep, short ranged attractive well (for small q), outside the hard core. Such potentials induce much stronger pair correlations at the same density than those with longer ranged attraction, say a Lennard-Jones fluid. In particular the ''stickiness'' leads to very high values of g_{cc} at contact, $R=\sigma_c^+$. At present there is no reliable procedure for incorporating such strong attraction-induced correlation effects into DFT and we have chosen to employ the crudest mean-field treatment of attractive forces. The (grand potential) functional that we minimize is a standard one [20]:

$$\Omega_V[\rho_c]=\mathcal{F}_{\rm HS}[\rho_c]+\tfrac{1}{2}\int d\mathbf{R}_1\int d\mathbf{R}_2\rho_c(\mathbf{R}_1)\rho_c(\mathbf{R}_2)\phi_{\rm att}(R_{12}) + \int d\mathbf{R}[\mu_c-V(\mathbf{R})]\rho_c(\mathbf{R}), \tag{35}$$

where μ_c is the chemical potential of the colloids and $V(\mathbf{R})\equiv v_c^{\rm ext}(z)+\phi_{\rm AO}^{\rm wall}(z)$ is the effective wall potential appropriate to the hard wall. We restrict consideration to fluid-like states (no spontaneous crystalline ordering) so that $\rho_c(\mathbf{R})\equiv\rho_c(z)$. $\mathcal{F}_{\rm HS}[\rho_c]$ is the intrinsic free energy functional of the hard sphere fluid for which we use the fundamental measures theory of Rosenfeld [21]. The latter is known to be accurate for a wide variety of highly inhomogeneous situations [20,21]. A mean-field treatment leaves arbitrary the specification of the attractive pair potential $\phi_{\rm att}(R)$ inside the hard core. In order to mimic some effects of correlations we set

$$\phi_{\rm att}(R)=\begin{cases}\phi_{\rm AO}(R), & R>\sigma_c\\ \phi_{\rm AO}(\sigma_c), & 0<R\leqslant\sigma_c.\end{cases} \tag{36}$$

Such a choice yields a reasonable bulk free energy density and we checked that other choices, e.g., setting $\phi_{\rm att}(R)=0$ for $0<R<\sigma_c$, do not lead to dramatically different colloid profiles at the hard wall.

The Euler-Lagrange equation obtained from $\delta\Omega_V[\rho_c]/\delta\rho_c(z)=0$ was solved by Picard iteration for given bulk colloid density and given polymer fugacity z_p. We present results for state points specified by the bulk packing fractions $\eta_c=\pi\rho_c(\infty)\sigma_c^3/6$ and $\eta_p^r=\pi\rho_p^r\sigma_p^3/6$ with $\rho_p^r=z_p$.

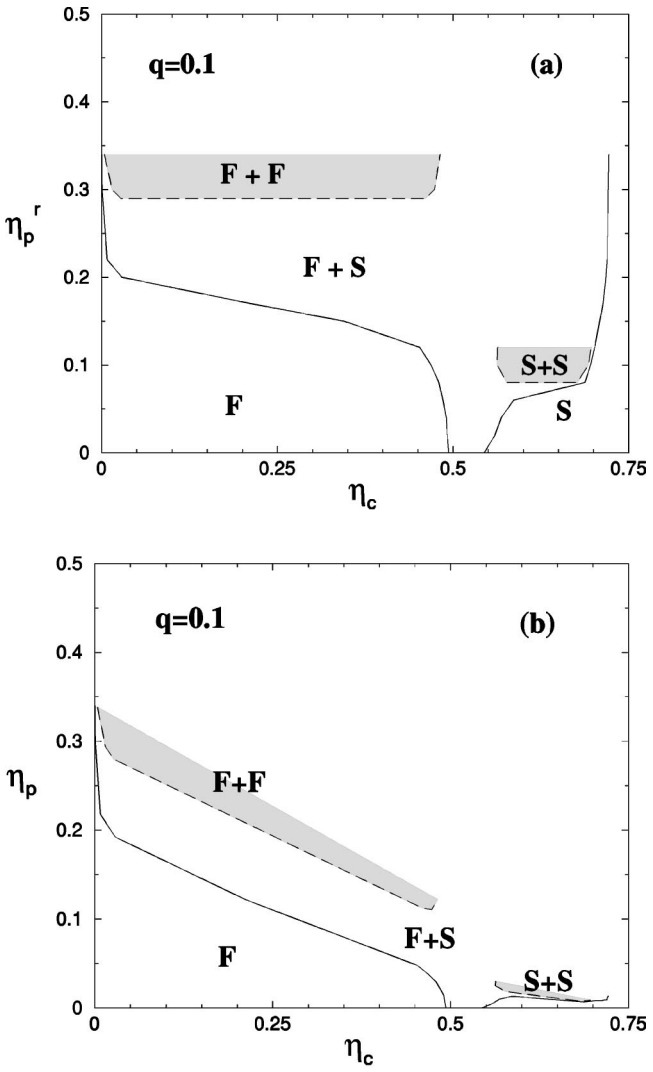

FIG. 3. The simulation phase diagram for a system of colloids interacting via the effective one-component Hamiltonian, i.e., the Asakura-Oosawa pair potential (11) for a size ratio $q\equiv\sigma_p/\sigma_c=0.1$ [3]. In (a) η_c is the colloid packing fraction and η_p^r is the packing fraction of ideal polymer in the reservoir. In (b) we plot the phase diagram in terms of η_c and η_p, the packing fraction of ideal polymer in the actual mixture given by the approximation $\eta_p/\eta_p^r=1-\eta_c(1+q)^3$. F and S denote the stable fluid and solid (fcc) phases while $F+S$, $F+F$, and $S+S$ denote, respectively, the stable fluid-solid, the metastable fluid-fluid, and the metastable solid-solid coexistence region.

We chose to study AO mixtures with $q=0.1$ since this is the only case, with $q<0.1547$, for which the bulk phase diagram has been determined fully by simulation [3]. The phase diagram is shown here in Fig. 3 and coexistence data is given in Table I. The fluid-fluid transition is strongly metastable with respect to a very broad, in η_c, fluid-solid coexistence for this size ratio. We deliberately avoid the bulk fluid-solid transition by restricting calculations to $\eta_p^r\leqslant 0.1$, i.e., to small polymer concentrations.

For comparison, we have also performed Monte Carlo simulations of the effective one-component system in which the colloids interact with a fluid-fluid pair potential $\phi_{cc}(R)$

TABLE I. The coexisting densities [expressed in terms of packing fractions of colloid (η_c) and ideal polymer (η_p)] at the stable fluid-solid, metastable fluid-fluid, and weakly metastable solid-solid transitions for a bulk colloid-polymer mixture with size ratio $q=0.1$ and varying reservoir polymer packing fractions η_p^r as determined by Monte Carlo simulation [3]. The polymer packings η_p in the actual mixture were calculated from the formula $\alpha=\eta_p/\eta_p^r=1-\eta_c(1+q)^3$.

Fluid-solid				
η_p^r	η_c (fluid)	η_p (fluid)	η_c (solid)	η_p (solid)
0.00	0.494	0.000	0.545	0.0000
0.02	0.492	0.007	0.560	0.0051
0.04	0.491	0.014	0.569	0.0097
0.06	0.486	0.021	0.587	0.0131
0.08	0.480	0.029	0.688	0.0067
0.10	0.469	0.038	0.696	0.0074
0.12	0.453	0.048	0.702	0.0079
0.15	0.345	0.081	0.709	0.0084
0.17	0.212	0.122	0.714	0.0084
0.20	0.029	0.192	0.718	0.0089
0.22	0.008	0.218	0.720	0.0092
0.30	6.2*E*-4	0.300	0.721	0.0121
0.34	7.9*E*-5	0.340	0.722	0.0133
Solid-solid				
η_n^r	η_c (solid 1)	η_p (solid 1)	η_c (solid 2)	η_p (solid 2)
0.08	0.577	0.0186	0.677	0.0079
0.10	0.563	0.0251	0.693	0.0078
0.12	0.564	0.0299	0.697	0.0087
Fluid-fluid				
η_p^r	η_c (fluid 1)	η_p (fluid 1)	η_c (fluid 2)	η_p (fluid 2)
0.29	0.027	0.2796	0.461	0.1121
0.30	0.015	0.2940	0.474	0.1107
0.34	0.004	0.3382	0.482	0.1219

$+\phi_{\rm AO}(R)$ and an effective wall potential $V(\mathbf{R})\equiv v_c^{\rm ext}(z)+\phi_{\rm AO}^{\rm wall}(z)$. In order to investigate the adsorption properties of the fluid, it is important to study the fluid in contact with a *single* wall. Here we use a simulation method in which the planar hard wall is located at $z=0$ and a self-consistently determined density $\rho_c(\infty)$ is imposed far from the hard wall, using a penalty function that suppresses large deviations from $\rho_c(\infty)$ and, hence, ensures a flat density profile. More details on this simulation method are given in Ref. [22]. Simulations are performed using 1920 particles in a box of lateral dimensions $L_x/\sigma_c=8.8606$, $L_y/\sigma_c=9.5919$, and $L_z/\sigma_c=30.44$ or $L_z/\sigma_c=40.15$, for $\eta_c=0.40$ and $\eta_c=0.30$, respectively. More than 5×10^4 Monte Carlo sweeps were allowed for equilibration and the density profiles were accumulated over a further 5×10^5 sweeps (one sweep is one attempted move per particle).

The effects on the colloid profile of adding polymer are very pronounced as is illustrated in Fig. 4 for $\eta_c=0.3$. In the absence of polymer, $\eta_p^r=0$ [see Fig. 4(a)], the system reduces to hard spheres at a hard wall for which the Rosenfeld functional performs very well. The results of DFT and the

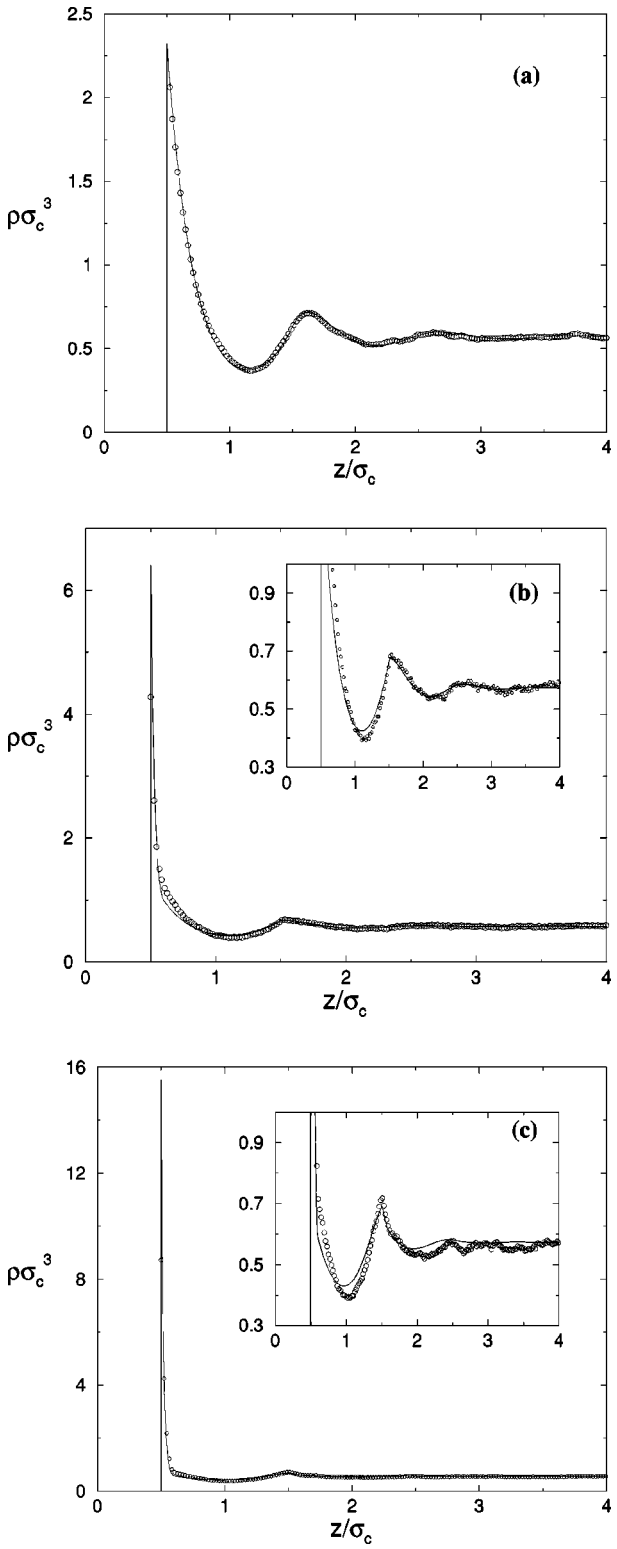

FIG. 4. Colloid density profiles near a hard wall: the open circles are the Monte Carlo results while the solid lines denote the DFT results. In each case the bulk colloid packing fraction $\eta_c=0.3$ and the size ratio $q=0.1$. The packing fraction of ideal polymer in the reservoir increases from (a) $\eta_p^r=0$ (pure hard spheres) to (b) $\eta_p^r=0.05$ and (c) $\eta_p^r=0.10$. The insets show the results on an expanded vertical scale. Note the rapid increase in contact value $\rho_c(\sigma_c^+/2)$ as η_p^r is increased.

present simulation are almost indistinguishable. On adding a very small amount of polymer, $\eta_p^r = 0.05$, the wall-induced depletion leads to a much higher value of the (reduced) contact density, $\rho_{wc}\sigma_c^3 \approx 6.41$ as compared with 2.32 for hard spheres at a hard wall. On the scale of Fig. 4(b) there is good agreement between theory and simulation. When the scale is expanded (see inset) there are differences, which we shall return to below.

Figure 4(c) displays the results for $\eta_p^r = 0.1$. Now the effect of depletion is even more pronounced and the (reduced) contact density from DFT increases to 15.52. Once again the overall agreement with simulation is good. Note that the (reduced) colloid density profiles decay rapidly from the very high contact values to values of about unity over the range $\sigma_p = 0.1\sigma_c$ of the wall depletion potential $\phi_{\mathrm{AO}}^{\mathrm{wall}}$. This means that the amount adsorbed in the contact ''layer'' remains a fraction of a colloid monolayer. The colloid is responding (essentially) as an ideal gas in the deep wall depletion potential. Indeed, the large contact densities can be accounted for qualitatively by the ideal gas result $\rho_{wc}\sigma_c^3 = \rho_c(\infty)\sigma_c^3 \exp[-\beta\phi_{\mathrm{AO}}^{\mathrm{wall}}(\sigma_c)]$ plus some small enhancement from packing effects. There is no evidence for any wall-induced local crystallization at these polymer concentrations. The colloid density at the first minimum of the profile is not substantially different from the bulk density $\rho_c(\infty)$. Figure 5 shows the corresponding results for $\eta_c = 0.4$. The bulk hard sphere fluid is closer to freezing ($\eta_{cf} = 0.494$) and the ordering of hard spheres at the hard wall is more pronounced [see Fig. 5(a)]. The Rosenfeld functional still provides an excellent account of the density profile at this higher packing fraction. As polymer is added the variation in the profiles is similar to that for the lower packing fraction of colloids. The contact densities become even higher for a given η_p^r; DFT gives $\rho_{wc}\sigma_c^3 \approx 27.64$ for $\eta_p^r = 0.1$. This implies that the packing effects are much more significant at $\eta_c = 0.4$. The level of agreement with simulation is similar to that for $\eta_c = 0.3$ and the DFT appears to capture all the main features in the shape of the colloid profiles. These are nontrivial as can be seen from the insets to Figs. 4 and 5. On increasing η_p^r at fixed η_c the minima in $\rho_c(z)$ shift to smaller z and the oscillations appear to decay more rapidly. Whether these features can be accounted for by the general theory of asymptotic decay of density profiles [23] remains to be ascertained. The amount adsorbed in the contact layer remains quite small for $\eta_c = 0.4$ and, as for $\eta_c = 0.3$, at the first minimum in the density profile the colloid density remains substantial, typically about half the bulk value. We checked the numerics of the DFT calculations by comparing the contact values ρ_{wc} with those resulting from Eq. (30), with the osmotic pressure Π obtained from the bulk free energy given by the DFT, Eq. (35). The results agree to better than 0.15% in all cases.

Performing Monte Carlo simulations for the strongly attractive and very short ranged potentials that arise for $q = 0.1$ and $\eta_p^r = 0.1$ is not straightforward. In Monte Carlo simulations, we select a particle at random and give it a random displacement. Usually the size of the displacement is chosen so that about 50% of the attempted moves are ac-

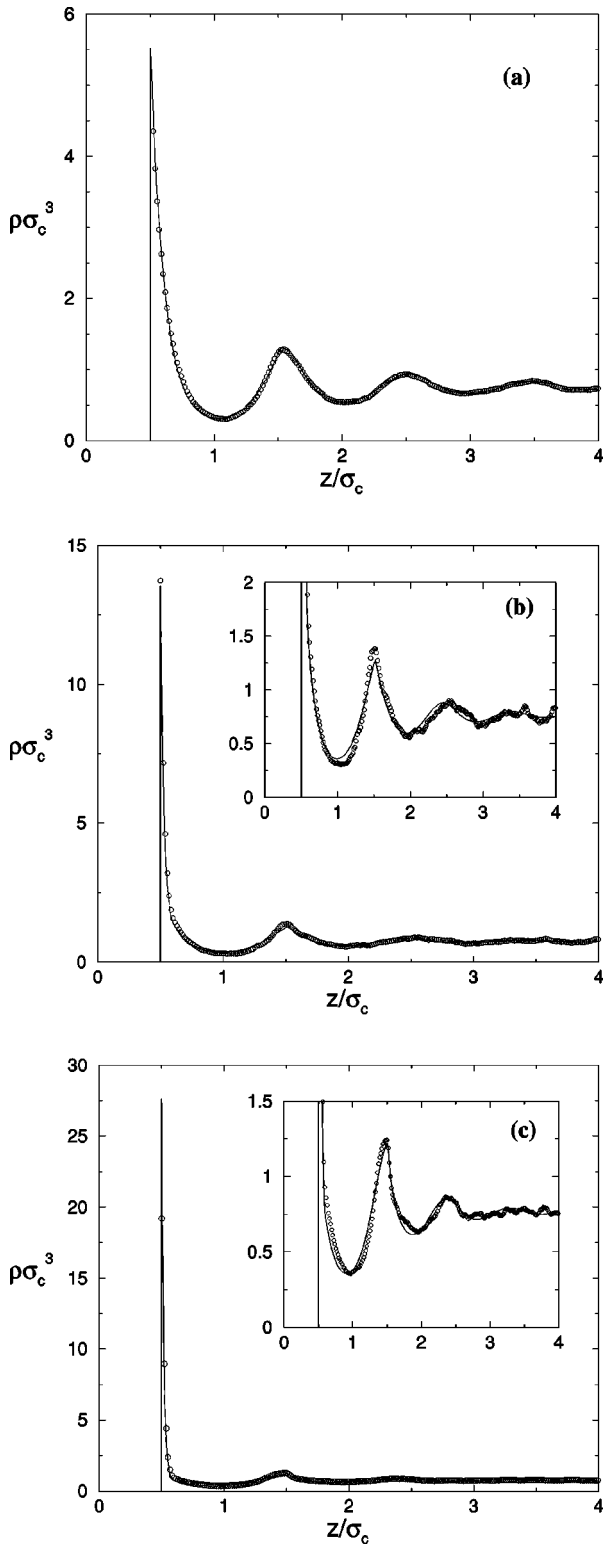

FIG. 5. Colloid density profiles near a hard wall: the open circles are the Monte Carlo results while the solid lines denote the DFT results. In each case the bulk colloid packing fraction $\eta_c = 0.4$ and the size ratio $q = 0.1$. The packing fraction of ideal polymer in the reservoir increases from (a) $\eta_p^r = 0$ (pure hard spheres) to (b) $\eta_p^r = 0.05$ and (c) $\eta_p^r = 0.10$. The insets show the results on an expanded vertical scale. Note the rapid increase in contact value $\rho_c(\sigma_c^+/2)$ as η_p^r is increased.

cepted. However, in an inhomogeneous system the acceptance probability is not uniform throughout the system. For instance, in a system with a strongly attractive and very short ranged wall-particle potential, as in our case, the acceptance probability is much lower close to the wall than in bulk. In order to obtain good statistics close to the wall, we must choose the size of the random displacements to be many times smaller than in bulk, corresponding to a higher overall acceptance probability. The drawback of such a high acceptance rate is that long simulation runs are needed for good statistical accuracy in the bulk. In the present simulations we have chosen the acceptance probability so that equally good statistics are obtained close to the wall as in bulk. This probability is about 75%. If we increase the acceptance probability, i.e., make smaller displacements, we find that the value of the contact density increases and the width of the first peak of the colloid density profiles decreases—moving toward the DFT results. However, simultaneously, the statistics for the second peak and for bulk become very poor, making difficult any fine comparison between theory and simulation.

V. DISCUSSION

In this paper we have developed a formal procedure for integrating out the degrees of freedom of the polymer in an inhomogeneous model colloid polymer mixture defined by Eqs. (1) and (2), the Asakura-Oosawa model Hamiltonian. For highly asymmetric mixtures, with size ratio $q<0.1547$, near a planar hard wall the resulting effective one-component Hamiltonian takes a particularly simple form, which is readily amenable to simulation studies and to investigation by one-component DFT. Our procedure enables us to map (exactly) a difficult binary mixture problem to its more tractable one-component counterpart. As an illustration of the procedure we have considered the adsorption for a binary mixture with $q=0.1$ at a planar hard wall at two different values of the colloid packing fraction η_c. In both cases, adding small amounts of polymer gives rise to deep depletion potentials at the wall, which yield, in turn, very high values of the colloid density near contact. The simple DFT, which treats the attractive part of the effective colloid-colloid pair potential in mean-field fashion, provides a good description of the main features of the colloid density profile. There are discrepancies between DFT and simulation but these are not large. The DFT does account for the very high contact values that are observed in the simulations. It is important to emphasize that for the range of polymer reservoir packing fractions we consider, i.e., η_p^r up to 0.1, the Gibbs adsorption $\Gamma=\int_0^\infty dz[\rho_c(z)-\rho_c(\infty)]$ does not increase rapidly with increasing η_p^r. Although the colloid density is strongly enhanced very close to the wall, i.e., within the narrow range of the wall depletion potential, this is insufficient to lead to pronounced increases in Γ. Moreover, the colloid density at the first minimum remains about half the bulk density so there is no indication of wall-induced local crystallization up to $\eta_p^r=0.1$. We note that these state points are still well removed from the bulk fluid-solid phase boundary (see Fig. 3). Whether wall-induced crystallization sets in at slightly higher polymer packing or whether one must approach very close to the bulk phase boundary in order to observe such a phenomenon remains to be investigated thoroughly. One might certainly expect depletion effects to favor the development of crystalline layers prior to bulk crystallization. The main issues are (i) how close to the bulk transition must one be before the first adsorbed layer becomes crystalline and (ii) how do subsequent crystalline layers develop at the hard wall-fluid interface as η_p^r is increased (for a fixed η_c) toward its value at bulk fluid-solid coexistence? Various scenarios are possible. There could be an infinite sequence of layering transitions culminating in complete wetting of the wall-fluid interface by a near close packed crystal. Alternatively, the interface could remain partially wetted by crystal. We should recall that the adsorption characteristics of pure hard spheres at a planar hard wall remain uncertain in the approach to the freezing transition—this corresponds to increasing η_c along the axis $\eta_p^r=0$ in Fig. 3 toward the value $\eta_c=0.494$ where bulk freezing occurs. One still does not know whether the hard wall–hard sphere fluid interface is completely wetted by hard sphere crystal [24].

Similar depletion phenomena should be found for additive binary mixtures of hard spheres near a hard wall, provided the size ratio q is small enough. DFT calculations for $\eta_c=0.3$ and 0.4 with a similar range of small sphere packing fractions based on the Rosenfeld functional for a binary mixture with $q=0.1$ yield big sphere (colloid) density profiles that are very similar to those shown here [25]. Once again there is no sign of crystallization at the wall for the state points that were investigated. Detailed comparisons of results for additive hard sphere mixtures with those from the AO model will be presented elsewhere but we remark that our findings are different from those of Poon and Warren [26], who developed an empirical approach for the calculation of the onset of wall crystallization in additive binary hard sphere mixtures. These authors find hard-wall-induced crystallization at small sphere packing fractions that are far below the bulk fluid-solid transition obtained in Ref. [12]. Our present results and those in Ref. [25] show no sign of wall-induced crystallization at state points where Ref. [26] predicts such a transition. These observations are relevant to experiments. Several papers [27–29] report evidence for wall-induced crystallization well below the bulk fluid-solid phase boundary in mixtures of hard-sphere-like colloids at a planar wall. There are also earlier observations of wall-induced crystallization in colloid-polymer mixtures [30,31]. How well the idealized model of the AO binary mixture near a planar hard wall mimics the experimental situations remains to be ascertained but our present theoretical framework does allow us to investigate these problems—at least for systems with size ratio $q<0.1547$.

The analysis presented in Sec. III focused on a planar hard wall. It is straightforward to generalize to a curved hard wall and it might be possible to develop the theory for structured walls, i.e., patterned substrates. Recent experiments [32] have shown that a variety of low-dimensional colloidal fluid and solidlike phases can develop for colloid polymer mixtures adsorbed on periodically patterned templates. En-

tropic depletion forces are responsible for the rich phase behavior.

We conclude by returning to the situation of spontaneously generated inhomogeneity where the one-body density profiles are spatially varying in the absence of external potentials. As emphasized earlier, for such situations the effective Hamiltonian $H^{\rm eff}$ reduces to that of the bulk system and for $q < 0.1547$ $H^{\rm eff} = \Omega_0^{\rm bulk} + \Omega_1^{\rm bulk} + H_{cc} + \Sigma_{i<j}\phi_{\rm AO}(R_{ij})$, where $\Omega_0^{\rm bulk} + \Omega_1^{\rm bulk}$ depend only on z_p, the fugacity of the reservoir. This implies that the properties of the interfaces between coexisting phases at a given z_p are determined solely by the pair potential $\phi_{cc}(R) + \phi_{\rm AO}(R)$ evaluated at that value of z_p. Thus one may calculate density profiles and surface tension at the fluid-solid interfaces and at the (metastable) solid-solid and fluid-fluid interfaces that arise between the phases indicated in Fig. 3 using the pair potential description. This illustrates further the usefulness of the mapping to an effective one-component system for highly asymmetric mixtures. For mixtures with $q > 0.1547$, where integrating out yields many-body contributions to the effective Hamiltonian, the mapping loses some of its appeal for calculational purposes. An alternative DFT approach specifically designed for the *binary* AO mixture, which can describe inhomogeneous mixtures with arbitrary size ratio, has been developed [33]. This DFT has been applied to the present problem of adsorption at a hard wall. Results will be presented elsewhere.

ACKNOWLEDGMENTS

We thank R. Roth, R. van Roij, and M. Schmidt for stimulating discussions and P. B. Warren for helpful correspondence. This research was supported by the EPSRC under Grant No. GR/L89013. M. D. is grateful to FOM for support under stimulerings programma.

[1] S. Asakura and F. Oosawa, J. Chem. Phys. **22**, 1255 (1954); J. Polym. Sci. **33**, 183 (1958).
[2] A. Vrij, Pure Appl. Chem. **48**, 471 (1976).
[3] M. Dijkstra, J. M. Brader, and R. Evans, J. Phys.: Condens. Matter **11**, 10 079 (1999).
[4] A. P. Gast, C. K. Hall, and W. B. Russel, J. Colloid Interface Sci. **96**, 251 (1983).
[5] H. N. W. Lekkerkerker, W. C. K. Poon, P. N. Pusey, A. Stroobants, and P. B. Warren, Europhys. Lett. **20**, 559 (1992).
[6] A. A. Louis, R. Finken, and J. P. Hansen, Europhys. Lett. **46**, 741 (1999).
[7] M. Dijkstra, R. van Roij, and R. Evans, J. Chem. Phys. **113**, 4799 (2000).
[8] Surface tension studies reported by E. H. A. de Hoog and H. N. W. Lekkerkerker [J. Phys. Chem. B **103**, 5274 (1999)] and by G. A. Vliegenthart and H. N. W. Lekkerkerker [Prog. Colloid Polym. Sci. **105**, 27 (1997)].
[9] E. H. A. de Hoog, H. N. W. Lekkerkerker, J. Schulz, and G. H. Findenegg, J. Phys. Chem. B **103**, 10 657 (1999).
[10] J. M. Brader and R. Evans, Europhys. Lett. **49**, 678 (2000).
[11] J. P. Hansen and I. R. McDonald, *Theory of Simple Liquids* (Academic, London, 1986).
[12] M. Dijkstra, R. van Roij, and R. Evans, Phys. Rev. E **59**, 5744 (1999).
[13] An infinitesimal (gravitational) field is required to stabilize such an interface.
[14] R. Evans, Adv. Phys. **28**, 143 (1979).
[15] The procedure used to calculate the free energy in the Monte Carlo simulations of Ref. [3] is equivalent to utilizing Eq. (22).
[16] J. M. Brader (unpublished).
[17] H. Reiss, H. L. Frisch, and J. L. Lebowitz, J. Chem. Phys. **31**, 369 (1959); J. L. Lebowitz, E. Helfand, and E. Praestgaard, *ibid.* **43**, 774 (1965).
[18] P. Tarazona and R. Evans, Mol. Phys. **52**, 847 (1984); F. van Swol and J. R. Henderson, Phys. Rev. A **40**, 2567 (1989).
[19] G. Rickayzen, Mol. Phys. **55**, 161 (1985).
[20] R. Evans, in *Fundamentals of Inhomogeneous Fluids*, edited by D. Henderson (Dekker, New York, 1992), Chap. 3, and references therein.
[21] Y. Rosenfeld, Phys. Rev. Lett. **63**, 980 (1989); J. Chem. Phys. **98**, 8126 (1993).
[22] M. Dijkstra, R. van Roij, and R. Evans, Phys. Rev. E (to be published).
[23] R. Evans, J. R. Henderson, D. C. Hoyle, A. O. Parry, and Z. A. Sabeur, Mol. Phys. **80**, 755 (1993); R. Evans, R. J. F. Leote de Carvalho, J. R. Henderson, and D. C. Hoyle, J. Chem. Phys. **100**, 591 (1994).
[24] M. Dijkstra (unpublished); M. Heni and H. Löwen (unpublished).
[25] R. Roth (private communication).
[26] W. C. K. Poon and P. B. Warren, Europhys. Lett. **28**, 513 (1994).
[27] P. D. Kaplan, J. L. Rouke, A. G. Yodh, and D. J. Pine, Phys. Rev. Lett. **72**, 582 (1994).
[28] A. D. Dinsmore, A. G. Yodh, and D. J. Pine, Phys. Rev. E **52**, 4045 (1995).
[29] A. D. Dinsmore, P. B. Warren, W. C. K. Poon, and A. G. Yodh, Europhys. Lett. **40**, 337 (1997).
[30] A. Kose and S. Hachisu, J. Colloid Interface Sci. **55**, 487 (1976).
[31] A. P. Gast, W. B. Russel, and C. K. Hall, J. Colloid Interface Sci. **109**, 161 (1986).
[32] K.-H. Lin, J. C. Crocker, V. Prasad, A. Schofield, D. A. Weitz, T. C. Lubensky, and A. G. Yodh, Phys. Rev. Lett. **85**, 1770 (2000).
[33] M. Schmidt, H. Löwen, J. M. Brader, and R. Evans, Phys. Rev. Lett. **85**, 1934 (2000).